

A BRUSH-TYPE DYNAMIC TIRE FRICTION MODEL FOR NON-UNIFORM NORMAL PRESSURE DISTRIBUTION

Joško Deur

*Faculty of Mechanical Engineering and Naval Architecture, University of Zagreb
I. Lučića 5, HR-10000 Zagreb, Croatia*

Abstract: A dynamic tire friction model based on the LuGre friction model has been developed recently. The model includes the longitudinal and lateral forces, as well as the self aligning torque. It has originally been derived in distributed form, and then transformed to simpler lumped form with only three internal states. The lumped model has been based on uniform normal pressure distribution. It is extended in this paper for the more realistic case of a non-uniform normal pressure distribution, in order to provide a consistent prediction of the self aligning torque static curves. *Copyright © 2002 IFAC*

Keywords: Tire, modeling, friction, vehicle dynamics, simulation.

1. INTRODUCTION

There has been a significant research interest in modeling of the tire friction dynamics in recent years. This interest has been motivated by two observations: (i) the tire friction dynamics may be important from the standpoint of development of high performance ABS, traction control, and vehicle dynamics systems (van Zanten et al., 1989, 1990), and (ii) numerical difficulties of traditional static tire models at low vehicle speeds can be avoided by using a dynamic tire model (Bernard and Clover, 1995).

The distributed tire model, developed by van Zanten et al. (1989, 1990), captures all important aspects of the tire friction dynamics. However, it has a relatively complex, multi-state structure, and thus relatively low computing efficiency. A more pragmatic tire modeling approach has led to the relaxation length-based model (Bernard and Clover, 1995; Maurice et al., 1998), which can be regarded as a semi-empirical quasi-static lumped model.

Canudas de Wit and Tsiotras (1999) have proposed a new dynamic model for longitudinal tire force, which is based on the previously developed LuGre dynamic friction model. The model combines the advantages of the aforementioned dynamic tire models: it is originally expressed in the distributed ("brush") form, and it can be transformed into a simple lumped form. In addition, it

includes more accurate tire friction description than the brush model proposed by van Zanten et al. (1989, 1990), and has a compact form which is convenient for different tire dynamics analysis and estimation purposes.

Deur et al. (2000) and Deur (2001a) have modified the LuGre tire friction model, in order to provide consistent prediction of static tire characteristics. The modified model has then been extended for combined longitudinal and lateral motion, including calculation of the self aligning torque (Deur et al., 2001). The lumped model form has been derived based on the idealized assumption of uniform normal pressure distribution. However, the use of uniform normal pressure distribution has been found to be inadequate in view of obtaining accurate self aligning torque static curves. That has been motivation for developing a more general lumped tire friction model based on a non-uniform normal pressure distribution (Deur, 2001b), which is presented in the paper.

2. DISTRIBUTED MODEL

The tire coordinate system, including the main tire model quantities, is defined in Fig. 1 (Pacejka and Sharp, 1991). The tire friction dynamic behavior has been modeled in (Deur et al., 2001) based on the LuGre friction model and the following assumptions (cf. (Pacejka and Sharp, 1991; Clark, 1981)):

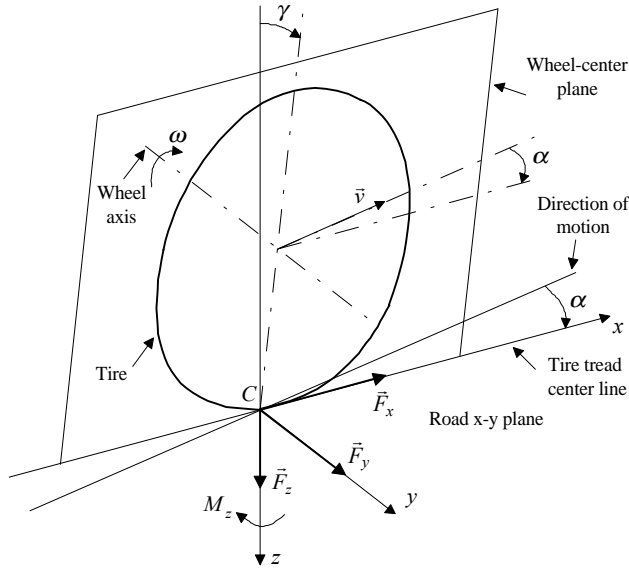


Fig. 1. Coordinate system of tire.

- The tire is represented in the region of contact with the road with a lot of tiny, massless and elastic bristles (so-called brush tire representation).
- The camber angle γ is equal to zero.
- Variation of the bristle slip speed along the tire/road contact length due to turning, camber, and deflection-variation effects is neglected.
- The tire/road contact patch has a rectangular form with the length L and width W .
- The normal pressure distribution along the lateral (y) axis is uniform.
- A non-uniform normal pressure distribution along the longitudinal (x) axis is incorporated in the model in a way which assumes proportional dependence of the bristle stiffness to the normal force F_z .
- A basic model for self aligning torque, with neglected residual torque and carcass compliance effects, is considered.

2.1 Dynamic model

The distributed dynamic tire friction model from (Deur et al., 2001) is defined by the following set of equations:

$$\frac{\partial z_{x,y}(\zeta, t)}{\partial t} = v_{rx,y} - \frac{\sigma_{0x,y} |v_r|}{g(v_r)} z_{x,y}(\zeta, t) - r |\omega| \frac{\partial z_{x,y}(\zeta, t)}{\partial \zeta} \quad (1)$$

$$\varphi_{x,y}(\zeta, t) = \bar{p}(\zeta) \frac{1}{LW} \left[\sigma_{0x,y} z_{x,y}(\zeta, t) + \sigma_{1(x,y)} \frac{\partial z_{x,y}(\zeta, t)}{\partial t} + \sigma_2 v_{rx,y} \right] \quad (2)$$

$$F_{x,y}(t) = \int_{-W/2}^{W/2} \int_0^L \varphi_{x,y}(\zeta, t) d\zeta dy = W \int_0^L \varphi_{x,y}(\zeta, t) d\zeta \quad (3)$$

$$M_z(t) = W \int_0^L \varphi_y(t) \left(\frac{L}{2} - \zeta \right) d\zeta \quad (4)$$

Eq. (1) describes the bristle horizontal deflection process in the longitudinal (x) and lateral (y) directions. The model states $z_{x,y}(\zeta, t)$ relate to the horizontal deflections of a bristle at the position ζ and time t through nonlinear functions which correspond to the bristle hysteretic stress-strain curves (Deur et al., 2000). The relative speeds (slip speeds) $v_{r(x,y)}$ are defined as

$$v_{rx} = r\omega - v \cos \alpha, \quad (5)$$

$$v_{ry} = v \sin \alpha, \quad (6)$$

$$v_r = \sqrt{v_{rx}^2 + v_{ry}^2}. \quad (7)$$

The tire/road sliding friction function g is given by

$$g(v_r) = F_C + (F_S - F_C) e^{-|v_r/v_s|^\delta}. \quad (8)$$

Eq. (2) describes the lateral and longitudinal components of tire force contribution of a bristle at the position ζ (defined per unit area of contact patch), where σ_0 and σ_1 are the bristle stiffness and damping coefficients, and σ_2 is the viscous friction coefficient. This tire force contribution is weighted by the normalized normal pressure $\bar{p}(\zeta)$. According to Eqs. (3) and (4), the total longitudinal and lateral forces $F_{x,y}$, and the self aligning torque M_z are obtained by integrating the tire forces and torque contributions over the total tire/road contact patch.

An asymmetric trapezoidal normal pressure distribution along the longitudinal (x) axis is assumed (Fig. 2, (Deur et al., 2001)). The normal pressure function $\bar{p}(\zeta)$ is given in a normalized (non-dimensional) form. Its mean value is set to one, so that it relates to the dimensional pressure variable $p(\zeta)$ as

$$\bar{p}(\zeta) = \frac{LW}{F_z} p(\zeta). \quad (9)$$

The magnitude \bar{p}_m of the normalized normal pressure function $\bar{p}(\zeta)$ is found to be (Deur et al., 2001; Fig. 2):

$$\bar{p}_m = \frac{2}{1 + r_r - r_l}. \quad (10)$$

with

$$r_{l,r} = \frac{\zeta_{l,r}}{L}. \quad (11)$$

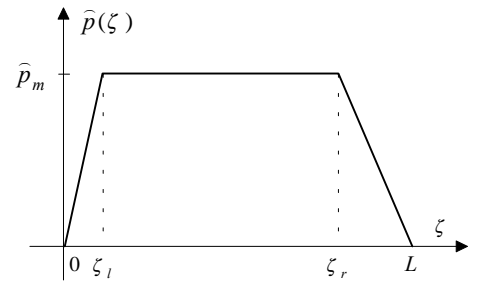


Fig. 2. Asymmetric trapezoidal normal pressure distribution.

2.2 Static model

The distributed dynamic tire friction model (1)-(4) has an analytical solution for the steady-state conditions. The steady-state (static) model relations, which have been derived in (Deur et al., 2001), are extended here for the case of non-zero viscous friction term $\sigma_2 v_{rx,y}$ in Eq. (2):

$$z_{x,y}(\zeta) = \text{sgn}(v_{rx,y}) \left| \frac{v_{rx,y}}{v_r} \right| \frac{g(v_r)}{\sigma_{0x,y}} \left(1 - e^{-\zeta/Z_{x,y}} \right), \quad (12)$$

$$F_{x,y} = \frac{v_{rx,y}}{v_r} g(v_r) \left\{ 1 - \frac{2}{1+r_r-r_l} \rho_{x,y} \left[\frac{\rho_{x,y}}{r_l} \left(1 - e^{-r_l/\rho_{x,y}} \right) - \frac{\rho_{x,y}}{1-r_r} \left(e^{-r_r/\rho_{x,y}} - e^{-1/\rho_{x,y}} \right) \right] \right\} + \sigma_2 v_{rx,y}, \quad (13)$$

$$M_z = \frac{v_{ry}}{v_r} g(v_r) \frac{L}{2} \left\{ 1 - K_v + \frac{2}{1+r_r-r_l} \rho_y^2 \left[\frac{4\rho_y-1}{r_l} - \frac{4\rho_y+2r_l-1}{r_l} e^{-r_l/\rho_y} - \frac{4\rho_y+2r_r-1}{1-r_r} e^{-r_r/\rho_y} + \frac{4\rho_y+1}{1-r_r} e^{-1/\rho_y} \right] \right\} + \frac{L}{2} (1-K_v) \sigma_2 v_{ry}, \quad (14)$$

with

$$K_v = \frac{2}{L^2} \int_0^L \zeta \widehat{p}(\zeta) d\zeta = \frac{2}{3} \frac{1+r_r+r_l^2-r_l^2}{1+r_r-r_l} = \widehat{p}_m \frac{1+r_r+r_l^2-r_l^2}{3} \quad (15)$$

$$\rho_{x,y} = \frac{Z_{x,y}}{L} = \frac{1}{L} \left| \frac{r\omega}{v_r} \right| \frac{g(v_r)}{\sigma_{0x,y}}. \quad (16)$$

3. LUMPED MODEL

3.1 Lumped model for longitudinal and lateral forces

The lumped model for longitudinal and lateral forces ($F_{x,y}$ -model) is defined in a pair of space-independent states $\tilde{z}_{x,y}(t)$, which are obtained by averaging deflection variables $z_{x,y}(\zeta, t)$ weighted by normalized normal pressure distribution $\widehat{p}(\zeta)$:

$$\tilde{z}_{x,y}(t) \stackrel{!}{=} \frac{1}{L} \int_0^L z_{x,y}(\zeta, t) \widehat{p}(\zeta) d\zeta. \quad (17)$$

Averaging the distributed $F_{x,y}$ -model (1)-(3) (by applying the integral $\frac{1}{L} \int_0^L (\cdot) \widehat{p}(\zeta) d\zeta$), and taking into account lumped state variables definition (17) yields

$$\frac{d\tilde{z}_{x,y}(t)}{dt} = v_{rx,y} - \frac{\sigma_{0x,y} |v_r|}{g(v_r)} \tilde{z}_{x,y}(t) - \frac{r|\omega|}{L} S_{x,y}(t), \quad (18)$$

$$F_{x,y}(t) = \sigma_{0x,y} \tilde{z}_{x,y}(t) + \sigma_{1(x,y)} \frac{d\tilde{z}_{x,y}(t)}{dt} + \sigma_2 v_{rx,y}. \quad (19)$$

with

$$S_{x,y}(t) = \int_0^L \frac{\partial z_{x,y}(\zeta, t)}{\partial \zeta} \widehat{p}(\zeta) d\zeta \quad (20)$$

All the terms in the model (18) and (19), except the term $S_{x,y}$ (Eq. (20)), have the lumped forms. The integral expression (20) can be solved in the discrete-space domain, as shown in Appendix A. The final solution is

$$S_{x,y}(t) = \widehat{p}_m \left(\frac{1}{L-\zeta_r} \int_{\zeta_r}^L z_{x,y}(\zeta, t) d\zeta - \frac{1}{\zeta_l} \int_0^{\zeta_l} z_{x,y}(\zeta, t) d\zeta \right). \quad (21)$$

In order to obtain a lumped model, the terms $S_{x,y}(t)$ need to be approximately expressed as functions of the lumped state variables $\tilde{z}_{x,y}(t)$. The simple proportional relation between these variables has been proposed in (Deur et al., 2000, 2001; Deur, 2001):

$$S_{x,y}(t) \approx \kappa_{x,y} \tilde{z}_{x,y}(t). \quad (22)$$

Hence, the state equation (18) assumes the following lumped form:

$$\frac{d\tilde{z}_{x,y}(t)}{dt} = v_{rx,y} - \left[\frac{\sigma_{0x,y} |v_r|}{g(v_r)} + \frac{\kappa_{x,y}}{L} r|\omega| \right] \tilde{z}_{x,y}(t). \quad (23)$$

The tire static curves (steady-state behavior) of the lumped model will be equal to those of the distributed model if the variable factors $\kappa_{x,y}$ are used (cf. (Deur et al., 2001)):

$$\kappa_{x,y} = \frac{S_{x,y}}{\tilde{z}_{x,y}} \Big|_{\text{steady state}} = \frac{\widehat{p}_m \left(\frac{1}{L-\zeta_r} \int_{\zeta_r}^L z_{x,y}(\zeta) d\zeta - \frac{1}{\zeta_l} \int_0^{\zeta_l} z_{x,y}(\zeta) d\zeta \right)}{\frac{1}{L} \int_0^L z_{x,y}(\zeta) \widehat{p}(\zeta) d\zeta} \quad (24)$$

Inserting Eq. (12) for the steady-state deflection variable space-distribution in Eq. (24), solving the integral expressions, and rearranging yields

$$\kappa_{x,y} = \frac{1}{\frac{1}{\widehat{p}_m E} - \rho_{x,y}}, \quad (25)$$

with

$$E = \frac{\rho_{x,y}}{r_l} \left(1 - e^{-r_l/\rho_{x,y}} \right) - \frac{\rho_{x,y}}{1-r_r} \left(e^{-r_r/\rho_{x,y}} - e^{-1/\rho_{x,y}} \right).$$

The factors $\kappa_{x,y}$ monotonically decrease with increase of the slip speed v_r . The boundary values of the factors $\kappa_{x,y}$ are found to be

$$\kappa_{\min} = \lim_{v_r \rightarrow \infty} \kappa_{x,y} = 0,$$

$$\kappa_{\max} = \lim_{v_r \rightarrow 0} \kappa_{x,y} = 2 \frac{(1+r_r-r_l)/2}{(r_r^2+r_r+1-r_l^2)/3}. \quad (26)$$

For large slip speeds (i.e. in the full-sliding operating regime), the factors $\kappa_{x,y}$ tend to zero, and the lumped tire friction model given by Eqs. (19) and (23) collapses to the standard LuGre friction model (given for a sliding pair). This is the correct result, which was not predicted by the lumped model with uniform normal pressure distribution (where $\kappa_{min} = 1$, (Deur, 2001)). However, the both models predict the similar results, since in the large slip operating regime the second term in the square bracket in Eq. (23) (so-called convective term) is much smaller (for any $\kappa \leq 1$) than the first term in the square bracket.

3.1 Lumped model for self aligning torque

In order to derive a lumped self aligning torque model, an additional lumped model state is introduced:

$$\psi(t) = \frac{2}{L} \frac{1}{L} \int_0^L \zeta z_y(\zeta, t) \bar{p}(\zeta) d\zeta. \quad (27)$$

Using the definitions (17) and (27), and Eqs. (2) and (15), the model output equation (4) is readily transferred to the lumped form

$$M_z(t) = \frac{L}{2} [\sigma_{0y} (\tilde{z}_y(t) - \psi(t)) + \sigma_{1(y)} \left(\frac{d\tilde{z}_y(t)}{dt} - \frac{d\psi(t)}{dt} \right) + (1 - K_v) \sigma_2 v_{ry}]. \quad (28)$$

On the other hand, averaging the distributed model lateral (y) state equation (1) (by applying the integral $\frac{2}{L^2} \int_0^L \zeta (\cdot) \bar{p}(\zeta) d\zeta$), and taking into account lumped state variable definition (27) and Eq. (15) yields

$$\frac{d\psi(t)}{dt} = K_v v_{ry} - \frac{\sigma_{0y} |v_r|}{g(v_r)} \psi(t) - \frac{2}{L} r |\omega| S(t), \quad (29)$$

with

$$S(t) = \frac{1}{L} \int_0^L \zeta \frac{\partial z_y(\zeta, t)}{\partial \zeta} \bar{p}(\zeta) d\zeta. \quad (30)$$

Solving the integral expression (30) in the discrete-space domain yields (Appendix A):

$$S(t) = -\tilde{z}_y(t) + S^*(t) \quad (31)$$

with

$$S^*(t) = \frac{\bar{p}_m}{L} \left(\frac{1}{L - \zeta_r} \int_{\zeta_r}^L z_y(\zeta, t) \zeta d\zeta - \frac{1}{\zeta_l} \int_0^{\zeta_l} z_y(\zeta, t) \zeta d\zeta \right) \quad (32)$$

In order to obtain a lumped model, the term $S^*(t)$ needs to approximately be expressed as a function of the lumped model states $\psi(t)$ and $\tilde{z}_y(t)$. The following simple linear relation between these variables is proposed:

$$S^*(t) \approx \lambda_1 \psi(t) + \lambda_2 \tilde{z}_y(t). \quad (33)$$

Taking into account Eqs. (31) and (33), the self aligning torque state equation (29) assumes the following lumped form:

$$\frac{d\psi(t)}{dt} = K_v v_{ry} - \left[\frac{\sigma_{0y} |v_r|}{g(v_r)} + \frac{2\lambda_1}{L} r |\omega| \right] \psi(t) + \frac{2}{L} (1 - \lambda_2) r |\omega| \tilde{z}_y(t) \quad (34)$$

The following special (basic) case of relation (33) was considered in (Deur et al., 2001):

$$S^*(t) \approx \lambda \psi(t). \quad (35)$$

In this case, in order to provide the correct steady-state model behavior, the factor λ is obtained as

$$\lambda = \frac{S^*}{\psi} \Bigg|_{\text{steady state}} = \frac{\frac{\bar{p}_m}{L} \left(\frac{1}{L - \zeta_r} \int_{\zeta_r}^L z_y(\zeta) \zeta d\zeta - \frac{1}{\zeta_l} \int_0^{\zeta_l} z_y(\zeta) \zeta d\zeta \right)}{\frac{2}{L} \frac{1}{L} \int_0^L \zeta z_y(\zeta) \bar{p}(\zeta) d\zeta} \quad (36)$$

Inserting Eq. (12) in Eq. (36), solving the integral expressions, and rearranging yields

$$\lambda = \frac{1 + \bar{p}_m \rho_y \left[\frac{\rho_y - \rho_y + r_l}{r_l} e^{-r_l/\rho_y} - \frac{\rho_y + r_r}{1 - r_r} e^{-r_r/\rho_y} + \frac{\rho_y + 1}{1 - r_r} e^{-1/\rho_y} \right]}{K_v - 2\bar{p}_m \rho_y^2 \left[\frac{2\rho_y - 2\rho_y + r_l}{r_l} e^{-r_l/\rho_y} - \frac{2\rho_y + r_r}{1 - r_r} e^{-r_r/\rho_y} + \frac{2\rho_y + 1}{1 - r_r} e^{-1/\rho_y} \right]} \quad (37)$$

The factor λ monotonically decreases with increase of the slip speed v_r , where the boundary values are found to be

$$\lambda_{\min} = \lim_{v_r \rightarrow \infty} \lambda = \frac{1}{K_v},$$

$$\lambda_{\max} = \lim_{v_r \rightarrow 0} \lambda = \frac{3}{2} \frac{(r_r^2 + r_r + 1 - r_l^2)/3}{(r_r^3 + r_r^2 + r_r + 1 - r_l^3)/4}. \quad (38)$$

In the case of uniform normal pressure distribution ($r_l = 0$, $r_r = 1$), the boundary values λ_{\min} and λ_{\max} take on the values 1 and 1.5, respectively.

If the more general relation (33) is used instead of Eq. (35), one of the factors λ_1 and λ_2 can be fixed to an arbitrary constant value. It has been shown by simulation, that the better results are obtained if the factor λ_2 is fixed to a constant value, with the factor λ_1 calculated to obtain the correct steady-state behavior:

$$\lambda_1 = \frac{L}{2} \frac{1}{r |\omega|} \left[\frac{\frac{2}{L} (1 - \lambda_2) r |\omega| \tilde{z}_y + K_v v_{ry}}{\frac{2}{L} r |\omega| \tilde{z}_y + K_v v_{ry}} - \left(\frac{\sigma_{0y} |v_r|}{g(v_r)} + \frac{2\lambda}{L} r |\omega| \right) - \frac{\sigma_{0y} |v_r|}{g(v_r)} \right]. \quad (39)$$

The final lumped tire friction model is given by Eqs. (23), (34), (19), and (28). It should be noted that the self aligning torque model is of second order for the difference of the first-order longitudinal/lateral force model (cf. (Maurice et al., 1998)).

4. MODEL VALIDATION

The developed lumped tire friction model is validated with respect to the original distributed LuGre tire model (1)-(4). The model parameters are listed in Appendix B. They have been obtained by optimization with respect to Pacejka static tire model (Deur et al., 2001).

Fig. 3 shows comparative responses of the lumped and distributed LuGre tire models to a series of slip angle steps during pure cornering, where the basic form of the self aligning torque model with $\lambda_1 = \lambda$ and $\lambda_2 = 0$ is used. Fig. 4 shows the comparative responses for different wheel center speeds v . Evidently, the lumped model responses preserve all basic characteristics of the original distributed model, which include:

- A characteristic flexion point of the self aligning torque response, which does not appear in the lateral force response (note that this difference is due to different orders of the $F_{x,y}$ and M_z -models, Section 3).
- A characteristic initial undershoot of the self aligning torque response. This effect reveals a non-minimum-phase nature of the M_z -model.
- Slow-down of the model response with decrease of the wheel speed. This effect may imply that the tire friction dynamics has larger impact to vehicle dynamics at lower vehicle speeds.

However, the lumped model response is slower than the response of the distributed model, particularly at lower slip angles α (up to 10% slower for F_y and up to 40% slower for M_z , according to the results of application of the flexion-tangent identification method). It was shown in (Deur et al., 2000) that the simple choice of constant factor $\kappa_{x,y} \approx 1.2$ improved the accuracy of longitudinal force dynamic response, but a relatively small steady-state error appeared in that case. It can be shown that the accuracy of self aligning torque dynamic model can also be improved by the choice of a constant factor λ , but the steady-state error becomes high in that case.

Fig. 5 illustrates the effects of introducing the factor $\lambda_2 \neq 0$ in the lumped form of self aligning torque model. This factor influences the initial delay (equivalent dead-time) and initial undershoot of the self aligning torque step response. The lumped model with $\lambda_2 = 0.2$ predicts more accurate initial part of the response compared to the basic lumped model with $\lambda_2 = 0$, while the choice $\lambda_2 = -0.4$ provides more accurate response settling time (cf. Figs. 5 and 3).

5. CONCLUSION

The lumped dynamic tire friction model proposed in (Deur et al., 2001) has been extended for the more general case of a non-uniform distribution of the normal pressure. The main advantage of the extended model is that it is capable to predict a correct steady-state behavior of the self aligning torque.

The lumped model validation has shown that the model preserves all the basic characteristics of the original distributed model. However, the pure cornering step response of the lumped model compared to the distributed

one is somewhat slower, particularly for low slip angles. Influence of this discrepancy to the dynamic error of overall vehicle dynamics/steering system simulation, as well as an experimental model validation, is planned to be addressed in future work.

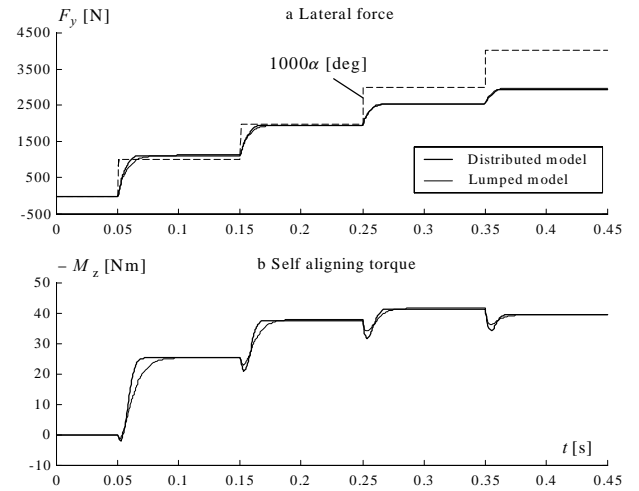


Fig. 3. Comparative pure cornering step responses of distributed and lumped tire models ($\lambda_2 = 0$).

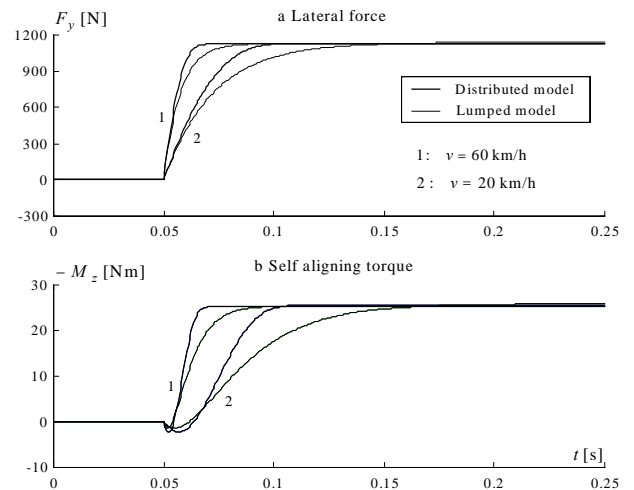


Fig. 4. Comparative pure cornering step responses for different wheel center speeds ($\alpha: 0 \rightarrow 1^\circ$ at 0.05 s).

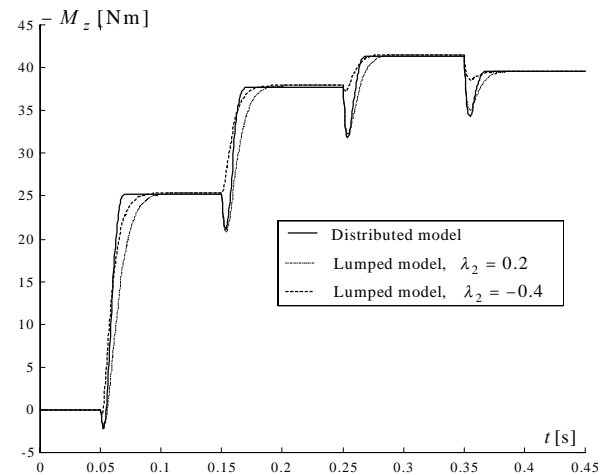


Fig. 5. Comparative pure cornering step responses for different factors λ_2 .

ACKNOWLEDGMENT

Support from Ford Motor Company and Ministry of Science and Technology of Republic of Croatia is gratefully acknowledged.

REFERENCES

- Bernard, J. E. and C. L. Clover (1995). Tire modeling for Low-Speed and High-Speed Calculations. *SAE paper #950311*.
- Canudas de Wit, C. and P. Tsiotras (1999). Dynamic Tire Friction Models for Vehicle Traction Control. *Proc. of 38th Conference on Decision and Control*, 3746-3751, Phoenix, Arizona, USA.
- Clark, S. K. (Ed.) (1981). *Mechanics of Pneumatic Tires*. U.S. Department of Transportation, NHTSA, Washington, D. C.
- Deur, J., J. Asgari and D. Hrovat (2000). Modeling and Analysis of Longitudinal Tire Dynamics. *FRL Technical report No. SRR-2000-0145*, Ford Motor Company, Dearborn, MI, USA.
- Deur, J. (2001a). Modeling and Analysis of Longitudinal Tire Dynamics Based on the LuGre Friction Model. *3rd IFAC Workshop Advances in Automotive Control*, 101-106, Karlsruhe, Germany.
- Deur, J., J. Asgari and D. Hrovat (2001). A Dynamic Tire Friction Model for Combined Longitudinal and Lateral Motion. *2001 ASME International Mechanical Engineering Congress and Exposition (IMECE 2001)*, CD-ROM Proceedings, Vol. 2, New York, NY, USA.
- Deur, J. (2001b). Lumped LuGre Tire Model for Non-uniform Normal Pressure Distribution. *Internal memorandum 04/13/01*, University of Zagreb, Croatia.
- Maurice J. P., M. Berzeri and H. B. Pacejka (1999). Pragmatic Tyre Model for Short Wavelength Side Slip Variations. *Vehicle System Dynamics*, **31**, pp. 65-94.
- Pacejka, H. B. and R. S. Sharp (1991). Shear Force Development by Pneumatic Tyres in Steady State Conditions: A Review of Modelling Aspects. *Vehicle System Dynamics*, **20**, 121-176.
- van Zanten, A., W. D. Ruf and A. Lutz (1989). Measurement and Simulation of Transient Tire Forces, *SAE paper #890640*.
- van Zanten, A., W. R. Erhardt and A. Lutz (1990). Measurement and Simulation of Transients in Longitudinal and Lateral Tire Forces, *SAE paper #900210*.

APPENDIX A. Derivation of terms $S_{x,y}$ and S

A.1 Term $S_{x,y}$

The term $S_{x,y}$, given by Eq. (20), can be rewritten in the discrete-space domain as (N -number of bristles; Fig. 2):

$$S_{x,y} = \lim_{N \rightarrow \infty} \sum_{i=1}^N \hat{p}_i [z_{x,yi} - z_{x,y(i-1)}] = \lim_{N \rightarrow \infty} (S_{1x,y} + S_{2x,y} + S_{3x,y})$$

with

$$S_{1x,y} = \sum_{i=1}^{N_l} K_l (i-1) (z_{x,yi} - z_{x,y(i-1)}) = -K_l \sum_{i=1}^{N_l-1} z_{x,yi} + K_l (N_l - 1) z_{x,yN_l}$$

$$S_{2x,y} = \hat{p}_m \sum_{i=N_l+1}^N (z_{x,yi} - z_{x,y(i-1)}) = -\hat{p}_m z_{x,yN_l} + \hat{p}_m z_{x,yN}$$

$$S_{3x,y} = -\sum_{i=N_r+1}^N K_r (i - N_r) (z_{x,yi} - z_{x,y(i-1)}) = K_r \sum_{i=N_r}^{N-1} z_{x,yi} - K_r (N - N_r) z_{x,yN}$$

and

$$K_l = \frac{\hat{p}_m}{N_l - 1}, \quad K_r = \frac{\hat{p}_m}{N - N_r}.$$

Rearranging the above equation for $S_{x,y}$ yields

$$S_{x,y} = \hat{p}_m \lim_{N \rightarrow \infty} \left(\frac{1}{N - N_r} \sum_{i=N_r}^{N-1} z_{x,yi} - \frac{1}{N_l - 1} \sum_{i=1}^{N_l-1} z_{x,yi} \right),$$

which can be rewritten in the continuous-space domain as Eq. (21).

A.2 Term S

The term S , given by Eq. (30), can be rewritten in the discrete-space domain as (Fig. 2):

$$S = \lim_{N \rightarrow \infty} \frac{1}{N} \sum_{i=1}^N (i-1) [z_{yi} - z_{y(i-1)}] \hat{p}_i = \lim_{N \rightarrow \infty} \frac{1}{N} (S_1 + S_2 + S_3)$$

with

$$S_1 = \sum_{i=1}^{N_l} K_l (i-1)^2 (z_{yi} - z_{y(i-1)}) = -K_l \sum_{i=1}^{N_l-1} (2i-1) z_{yi} + K_l (N_l - 1)^2 z_{yN_l}$$

$$S_2 = \hat{p}_m \sum_{i=N_l+1}^N (i-1) (z_{yi} - z_{y(i-1)}) = -\hat{p}_m \sum_{i=N_l+1}^{N-1} z_{yi} - \hat{p}_m N_l z_{yN_l} + \hat{p}_m (N-1) z_{yN}$$

$$\begin{aligned} S_3 &= -\sum_{i=N_r+1}^N K_r (i - N_r) (i-1) (z_{yi} - z_{y(i-1)}) = \\ &= K_r \sum_{i=N_r+1}^{N-1} (2i - N_r) z_{yi} + K_r N_r z_{yN_r} - K_r (N - N_r) (N-1) z_{yN}. \end{aligned}$$

Taking into account the discrete-space form of the lumped model state \tilde{z}_y (cf. Eq. (17))

$$\tilde{z}_y = \lim_{N \rightarrow \infty} \frac{1}{N} \left[K_l \sum_{i=1}^{N_l} (i-1) z_{yi} + \hat{p}_m \sum_{i=N_l+1}^N z_{yi} - K_r \sum_{i=N_r+1}^N (i - N_r) z_{yi} \right]$$

the above equation for the term S can be rearranged to

$$S = -\tilde{z}_y + S^*$$

with

$$S^* = \hat{p}_m \lim_{N \rightarrow \infty} \frac{1}{N} \left(\frac{1}{N - N_r} \sum_{i=N_r}^{N-1} i \tilde{z}_{yi} - \frac{1}{N_l - 1} \sum_{i=1}^{N_l-1} i \tilde{z}_{yi} \right).$$

The above equation for S^* can be transformed to the continuous-space domain as Eq. (32).

APPENDIX B. Parameters of tire friction model

$F_z = 4000$ N, $L\sigma_{0x} = 314 \cdot 10^3$ N, $L\sigma_{0y} = 159.2 \cdot 10^3$ N, $\sigma_1 = 0$, $\sigma_2 = 0$, $L = 0.303$ m, $F_C/F_z = 0.648$, $F_S/F_z = 1.671$, $v_s = 3.49$ m/s, $\delta_s = 0.6$, $r_l = 0.134$, $r_r = 0.707$, $N = 51$, $v = 60$ km/h.